

ARTICLES

Prediction of the new spinel phase of Ti_3N_4 and SiTi_2N_4 and the metal-insulator transition

W. Y. Ching,* Shang-Di Mo, and Lizhi Ouyang

Department of Physics, University of Missouri-Kansas City, Kansas City, Missouri, 64110

Isao Tanaka

Department of Energy Science and Technology, Kyoto University, Sakyo, Kyoto 606-8501, Japan

Masato Yoshiya

Department of Materials Science and Engineering, Kyoto University, Sakyo, Kyoto 606-8501, Japan

(Received 27 August 1999; revised manuscript received 5 November 1999)

Titanium nitrides are important materials with many industrial applications. However, the structure and properties of nitrogen-rich compounds are not well established. Based on *ab initio* calculations, stoichiometric titanium nitride compounds, *c*- Ti_3N_4 and *c*- SiTi_2N_4 , with a spinel structure were predicted. This result is different from the accepted model that TiN_x with $x > 1$ has a rocksalt structure with Ti vacancies. Electronic structure calculations show that these are highly covalent superhard materials. *c*- Ti_3N_4 is a narrow gap semiconductor and *c*- SiTi_2N_4 is a metal. By doping Ti at the octahedral site of the spinel *c*- Si_3N_4 , the direct band gap can be adjusted. An insulator-to-metal transition in *c*- $\text{Si}[\text{Si}_{1-x}\text{Ti}_x]_2\text{N}_4$ is predicted to occur at $x = 0.44$. A process of preparing these compounds is suggested, and several promising applications contemplated.

I. INTRODUCTION

Titanium compounds are widely used because of their many outstanding structural and electronic properties.¹ They can be metals, semiconductors, or ionic insulators depending upon the Ti valence state. Among them, TiC, TiN, and TiO_x with a rocksalt structure, exhibit extremely high hardness, high melting points, and chemical stability, and are referred to as refractory compounds.² Other than the rocksalt compounds, Ti_2O_3 and TiO_2 are the other well-known phases. Nonstoichiometry in the Ti compounds is common. For example, TiC_x with $0.47 < x < 0.95$, TiN_x with $0.39 < x < 1.0$ and TiO_x with $0.54 < x < 1.2$ are amply documented.³ These known Ti compounds are illustrated in Fig. 1 according to the formal valence of Ti. As can be noticed, the anticipated compound between Ti with a +4 valence or Ti (IV) and N which should have a chemical formula of Ti_3N_4 is conspicuously missing. Based on a critical review of 56 studies, Wriedt and Murray⁴ established the binary phase diagram of Ti-N for Ti:N ratio up to unity. There were several reports on the synthesis and properties of TiN_x films with $x > 1.0$ using techniques such as dual ion beam deposition,⁵ and metallorganic or inorganic precursor deposition.⁶⁻⁹ The generally accepted view is that these are TiN in rocksalt structure with vacancies at the metal sites.⁵ The existence (or nonexistence) of stoichiometric Ti_3N_4 compound is a subject of great scientific interest and technological significance.

The spinel phase is a major class of oxides with a chemical formula AB_2O_4 where A and B are the tetrahedral (tet) and octahedral (oct) cation sites. In a normal spinel such as MgAl_2O_4 , A has +2 valence and B has +3 valence. In the so-called inverse spinel, half of the B ions exchange sites

with the A ions to form $\text{B}[\text{AB}]\text{O}_4$. It is also possible to have mixed spinels of the form $(\text{A}_{1-2\lambda}\text{B}_{2\lambda})[\text{A}_{2\lambda}\text{B}_{2-2\lambda}]\text{O}_4$, where λ is the inversion parameter ranging from 0 for the normal spinel to 0.5 for the inverse spinel. The notable examples for inverse and the mixed spinels are Fe_3O_4 and $\text{Mg}_{0.1}\text{Fe}_{0.1}(\text{Mg}_{0.9}\text{Fe}_{1.1})\text{O}_4$, respectively.¹⁰ Recently, Zerr *et al.* reported the successful synthesis of spinel Si_3N_4 (*c*- Si_3N_4) by applying high-pressure and temperature of 15 GPa and 2000 K.¹¹ The occurrence of spinel nitrides with a formal anion valence of -3 is a significant discovery since it opens the door for an entirely new class of nitride compounds. Soon after the discovery, we have reported¹² that *c*- Si_3N_4 is a wide gap semiconductor having a direct band gap of 3.45 eV. We have also proposed that the transition pressure from hexagonal β - Si_3N_4 to the *c*- Si_3N_4 might be lowered by doping with Ti.

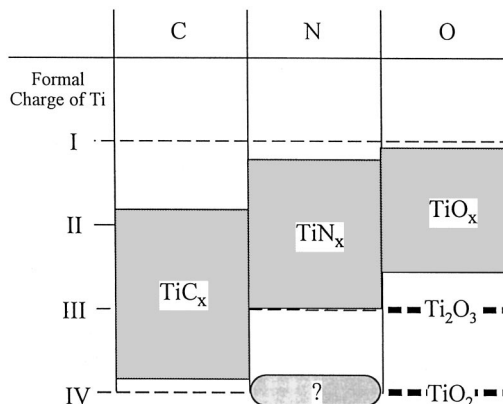


FIG. 1. Titanium compounds in various valence states.

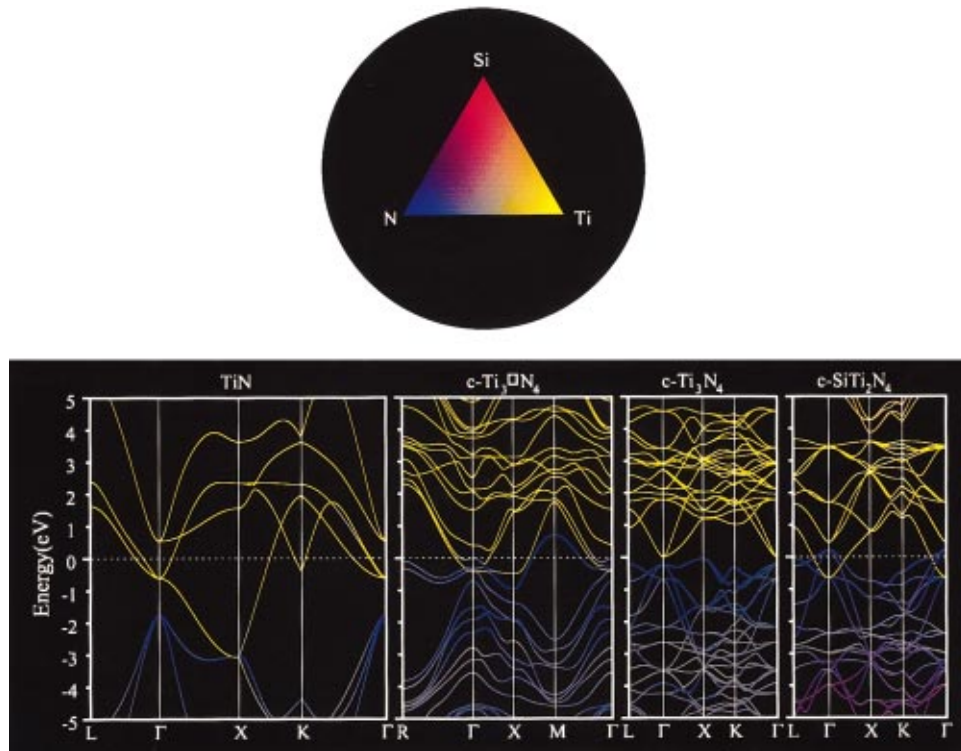


FIG. 2. (Color) Calculated band structure of (a) TiN; (b) $\text{Ti}_3\Box\text{N}_4$; (c) $c\text{-Ti}_3\text{N}_4$; (d) $c\text{-SiTi}_2\text{N}_4$. The color of each band is determined by the percentage of atomic origin as calculated from the wave function at each k point. The representations are red for Si, yellow for Ti, and blue for N. The color and the degree of mixing in the band is illustrated by the color triangle. So the orange bands above 4 eV in $c\text{-SiTi}_2\text{N}_4$ indicate a substantial mixing of Ti and Si orbitals. Likewise, the purple bands near -5 eV show interaction between N and Si. Note that the atomic components of the band can change along different k directions as a result of hybridization and the symmetry of the wave functions. The width of each panel is determined by the BZ of the crystal and is inversely proportional to the lattice constant.

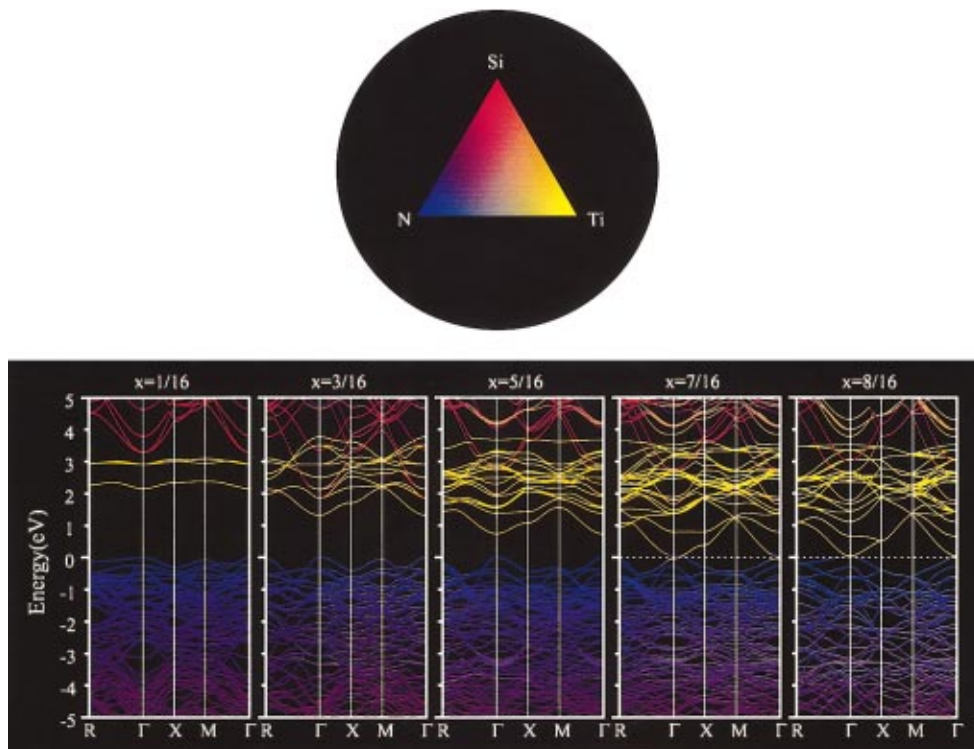


FIG. 5. (Color) Band structure for the solid solution $c\text{-Si}[\text{Si}_{1-x}\text{Ti}_x]_2\text{N}_4$ for $x = \frac{1}{16}$; $x = \frac{3}{16}$; $x = \frac{5}{16}$; $x = \frac{7}{16}$; $x = \frac{8}{16}$. The color designations are the same as in Fig. 2. Note the substantial mixing of Ti and Si in the CB.

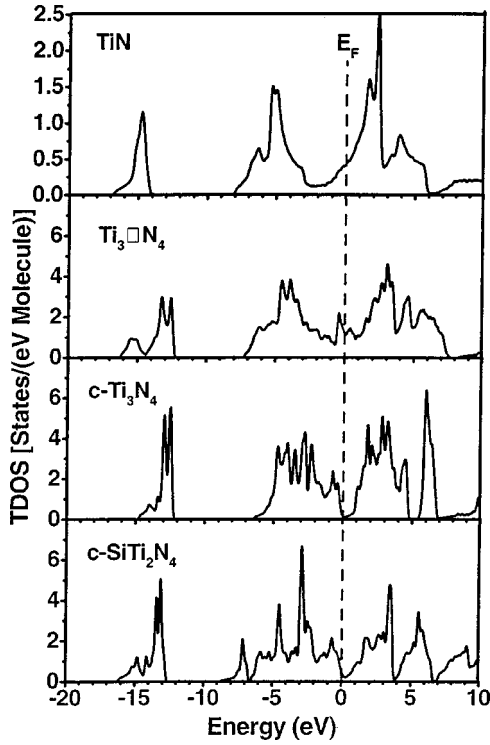


FIG. 3. Calculated DOS of A TiN; B $\text{Ti}_3\Box\text{N}_4$; C $c\text{-Ti}_3\text{N}_4$; D $c\text{-SiTi}_2\text{N}_4$. The zero of energy is set at the Fermi level for metal and at the top of VB for insulators.

Subsequent investigations lead us to the conclusion that spinel Ti_3N_4 ($c\text{-Ti}_3\text{N}_4$) should also exist. This further leads to the idea that mixed nitrides in the Si-Ti-N system should be stable. Indeed, we find that spinel SiTi_2N_4 (denoted as $c\text{-SiTi}_2\text{N}_4$ with Si at the tet site and Ti at the oct site) is stable but not vice versa. This implies that Si likes to be in a tet environment as in $\beta\text{-Si}_3\text{N}_4$ and Ti prefers an oct setting as in TiO_2 .

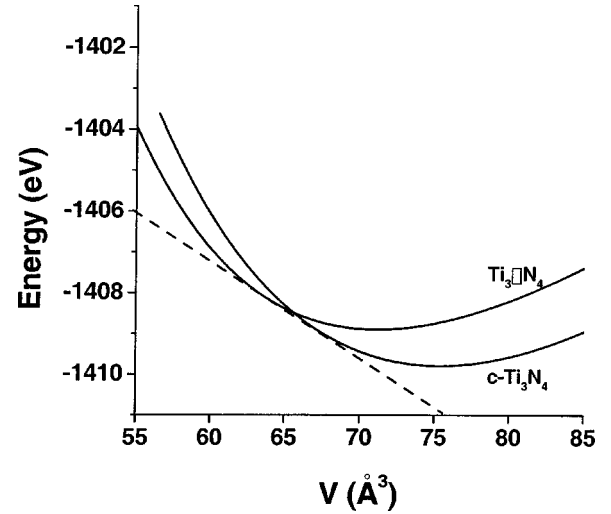


FIG. 4. Calculated total energy per Ti_3N_4 unit vs volume for $c\text{-Ti}_3\text{N}_4$ and $\text{Ti}_3\Box\text{N}_4$. The dashed line shows the possible transformation from $c\text{-Ti}_3\text{N}_4$ to $\text{Ti}_3\Box\text{N}_4$.

In the following section, we briefly outline our method and approach used in the prediction of these phases of nitrides and in the study of their properties. Our main results are presented in Sec. III. In Sec. IV, we discuss the possible ways of making these materials and also suggest several plausible applications in ceramic and semiconductor technologies. The paper ends with a succinct conclusion.

II. METHOD AND APPROACH

We used the first-principles orthogonalized linear combination of atomic orbitals (OLCAO) method¹³ within the local approximation of the density-functional theory¹⁴ for electronic structure and ground-state property calculations. A full basis set consisting of core orbitals of Si and N, valence electron orbitals of Si-3s, Si-3p, N-2s, and N-2p, and ad-

TABLE I. Calculated physical properties of $c\text{-Si}_3\text{N}_4$, $c\text{-Ti}_3\text{N}_4$, $\text{Ti}_3\Box\text{N}_4$, and $c\text{-SiTi}_2\text{N}_4$. a is the lattice constant and u is the internal parameter.

	$c\text{-Si}_3\text{N}_4$	$c\text{-Ti}_3\text{N}_4$	$\text{Ti}_3\Box\text{N}_4$	$c\text{-SiTi}_2\text{N}_4$
a (Å)	7.8367	8.4459	4.1327	8.2109
u	0.3843	0.3833	-	0.3758
Eq. Vol. ($\text{Å}^3/\text{mol}$)	60.160	75.309	70.535	69.196
E_g (eV)	3.45	0.25 (dir.) 0.07 (ind.)	metal	metal
Q^a (electron)				
Si or Ti (tet)	2.63	3.05	-	2.52
Si or Ti (oct)	2.54	3.22	3.11	3.31
N	6.05	5.63	5.54	5.72
Bond order ρ_{ij}				
Si or Ti (tet)-(N)	0.361	0.349	-	0.366
(bond length)	(1.830 Å)	(1.956 Å)	-	(1.790 Å)
Si or Ti (oct)-N	0.241	0.236	0.224 ^a	0.257
(bond length)	(1.885 Å)	(2.04 Å)	(2.076 Å) ^a	(2.045 Å)
Crystal bond order	8.670	8.465	8.048	9.094
B (GPa)	280	266	254	278

^aAveraged value.

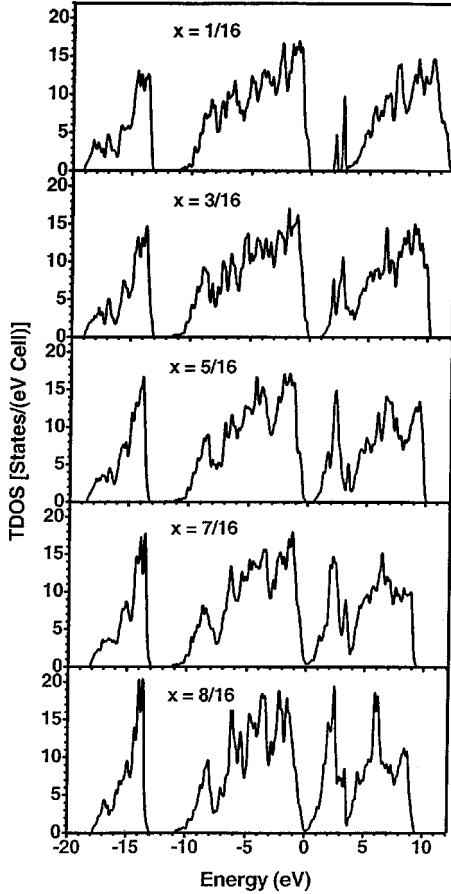


FIG. 6. DOS of $c\text{-Si}[\text{Si}_{1-x}\text{Ti}_x]_2\text{N}_4$ near the gap or the Fermi level for $x = \frac{1}{16}$; $x = \frac{3}{16}$; $x = \frac{5}{16}$; $x = \frac{7}{16}$; $x = \frac{8}{16}$.

ditional excited states orbitals (Si-4s, Si-4p, Si-3d, N-3s, N-3p) is employed. For each phase and composition, the total energy (TE) of the crystal is minimized by varying both the lattice constants and internal parameters. The computational procedure is the same as in Ref. 12 for $c\text{-Si}_3\text{N}_4$ and $c\text{-C}_3\text{N}_4$, except that in the present case much more k points in the irreducible part of the Brillouin zone (IBZ) must be used for metallic systems to achieve adequate convergence. We have used the same method to study the electronic structure of normal, inverse, and partially inverse spinels in the MgAl_2O_4 system.¹⁵ As a point of reference, our calculation predicts the lattice constant of TiN to within 0.1% of the measured value (4.241 Å). The TE of TiN converges to better than 0.0002 eV by using 250 k points in the IBZ. We used 44 and 68 k points in the IBZ for $c\text{-Ti}_3\text{N}_4$ and $c\text{-SiTi}_2\text{N}_4$, respectively for their TE calculations and geometry optimization. An important finding is that the final relaxed $c\text{-Ti}_3\text{N}_4$ structure is lower in energy than that of $3(\text{TiN}) + 0.5 \text{N}_2$ by 1.25 eV per Ti_3N_4 unit. This strongly suggests that the spinel phase is stable at least at low temperatures. To investigate the current defect model for Ti_3N_4 and TiN_x , we carried out the TE calculation of TiN in a rocksalt structure with an ordered Ti vacancy, which we denote as $\text{Ti}_3\Box\text{N}_4$. When fully relaxed and with a converged result using 68 k points in the IBZ, $\text{Ti}_3\Box\text{N}_4$ has a higher energy than $c\text{-Ti}_3\text{N}_4$ by about 0.93 eV per Ti_3N_4 unit, and the lattice constant reduces to 4.133 Å. The small difference in TE and equilibrium volume (see Table I) of the two

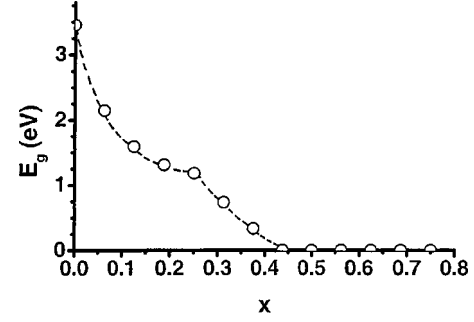


FIG. 7. x dependence of band gap E_g in $c\text{-Si}[\text{Si}_{1-x}\text{Ti}_x]_2\text{N}_4$. The calculated data points are based on a single configuration for each x . The dashed line is a guide to the eye.

phases indicates that the defect model may be valid for non-stoichiometric TiN_x films, but the stoichiometric $c\text{-Ti}_3\text{N}_4$ is a more stable compound. We further confirm that $c\text{-SiTi}_2\text{N}_4$ is more stable than a simple mixture of $1/3(c\text{-Si}_3\text{N}_4)$ and $2/3(c\text{-Ti}_3\text{N}_4)$ by 1.43 eV per SiTi_2N_4 formula unit. Thus $c\text{-SiTi}_2\text{N}_4$ should be an easily accessible compound.

The effective charges Q_α^* on each atom and the bond order $\rho_{\alpha,\beta}$ for each pair of atoms in the spinel crystals are calculated using the crystal wave functions and overlap integrals according to the Mulliken scheme.¹⁶

$$Q_\alpha^* = \sum_i \sum_{n,occ} \sum_{j,\beta} C_{i\alpha}^{*n} C_{j\beta}^n S_{i\alpha,j\beta}, \quad (1)$$

$$\rho_{\alpha\beta} = \sum_{n,occ} \sum_{i,j} C_{i\alpha}^{*n} C_{j\beta}^n S_{i\alpha,j\beta}. \quad (2)$$

Here $C_{i\alpha}^n$ is the coefficient for the eigenvector of state n with atomic specification α and orbital specification i . $S_{i\alpha,j\beta}$ is the overlap matrix between the Bloch functions. Separate calculations using a minimal basis set were invoked in order to be most effective in applying the Mulliken scheme.

To explore the properties of solid solutions between $c\text{-Si}_3\text{N}_4$, a wide-band-gap semiconductor and $c\text{-SiTi}_2\text{N}_4$, a metal, we used a ‘‘supercell’’ (the full cubic spinel cell) with 56 atoms for $c\text{-Si}[\text{Si}_{1-x}\text{Ti}_x]_2\text{N}_4$ and a progressive substitution of Si by Ti at the oct sites. In these fully self-consistent calculations, we used the scaled lattice constants and internal parameters between $c\text{-Si}_3\text{N}_4$ and $c\text{-SiTi}_2\text{N}_4$. Ideally, as many different substitutional configurations should be considered for each x , and the results averaged. Such extensive calculation is still quite prohibitive and a single representative configuration is used for each x .

III. RESULTS

The band structures of TiN, $\text{Ti}_3\Box\text{N}_4$, $c\text{-Ti}_3\text{N}_4$, and $c\text{-SiTi}_2\text{N}_4$ are shown in Fig. 2. We used a color graphic scheme for the bands $E_n(k)$ which can better illustrate the atomic origin and interatomic mixing for each band as k varies. (see caption of Fig. 2). In TiN, states within 1.7 eV of the Fermi level E_F are almost exclusively from Ti. For $c\text{-Ti}_3\text{N}_4$, the top of the valence band (VB) is at X consisting purely of the $N\text{-}2p$ nonbonding orbitals, and the bottom of the conduction band (CB) is at Γ with a small indirect band gap E_g of less than 0.1 eV. The direct E_g at Γ is 0.25 eV. In

contrast, $c\text{-Si}_3\text{N}_4$ has a direct E_g of 3.45 eV at Γ .¹² The fact that $c\text{-Ti}_3\text{N}_4$ is a semiconductor and TiN is a metal can be simply understood by the number of valence electrons per formula unit. The most conspicuous feature in TiN is an almost pure Ti band along $\Gamma\text{-}X$ extending down to 3 eV below E_F . The band structure of $\text{Ti}_3\Box\text{N}_4$ resembles neither TiN nor $c\text{-Ti}_3\text{N}_4$. There is a substantial portion of N -derived bands near the Fermi level. At the point M , a N -derived band actually crosses E_F . Despite the same formal charge, $c\text{-SiTi}_2\text{N}_4$ is a metal. From the colored band scheme, we can see that the metalization in $c\text{-SiTi}_2\text{N}_4$ is due to the increased Ti band width as the result of the modified interactions, such that the bottom of one of the Ti band overlap with the $N\text{-}2p$ band. The Fermi level E_F is slightly below the top of the VB at Γ , resulting in a small hole pocket. Doping with electron donor elements in $c\text{-SiTi}_2\text{N}_4$ may shift the E_F slightly up and eliminate the hole pocket at Γ . The color-coded scheme also shows that Si has little influence on the states near the Fermi level in $c\text{-SiTi}_2\text{N}_4$. The densities of states (DOS) of the four crystals are shown in Fig. 3. For TiN, our calculated DOS and band structure are the same as other recent *ab initio* calculations.^{17,18} In $c\text{-SiTi}_2\text{N}_4$, E_F lies near a minimum in the DOS which is an indication for the stability of the material. On the other hand, E_F in $\text{Ti}_3\Box\text{N}_4$ is near a local maximum in DOS.

The results for the effective charge and bond order calculations are listed in Table I. It is remarkable that the bond orders of Ti-N at both tet and oct sites are comparable to those of Si-N, in spite of the much longer Ti-N bonds. In particular, we find that $c\text{-SiTi}_2\text{N}_4$ has a higher crystal bond order (sum of all bond orders in the unit cell per molecular unit) than either $c\text{-Si}_3\text{N}_4$ or $c\text{-Ti}_3\text{N}_4$. This implies that with Si at the tet site and Ti at the oct site, an optimal bonding configuration is created. The defective $\text{Ti}_3\Box\text{N}_4$ has the lowest crystal bond order.

The bulk moduli B of the predicted crystals and that of $\text{Ti}_3\Box\text{N}_4$ are obtained by fitting the TE data to the Murnaghan equation of states and are listed in Table I. The TE at eight different crystal volumes were calculated with the internal parameter optimized in each case. $c\text{-Ti}_3\text{N}_4$ and $c\text{-SiTi}_2\text{N}_4$ have bulk moduli of 266 GPa and 278 GPa, respectively. These results again show that both spinel crystals are superhard materials with a high degree of covalent bonding. The bulk modulus for $\text{Ti}_3\Box\text{N}_4$ is somewhat smaller, 254 GPa, which is consistent with the smaller value of the crystal bond order. A common tangent construct to the TE vs volume curves as shown in Fig. 4 indicates that a transition from the $c\text{-Ti}_3\text{N}_4$ to $\text{Ti}_3\Box\text{N}_4$ may occur at about 35 GPa. This relatively high transition pressure is due to the rather close equilibrium volume of the two phases.

The band structures and DOS of $c\text{-Si}[\text{Si}_{1-x}\text{Ti}_x]_2\text{N}_4$ for a series of x values are shown in Figs. 5 and 6, respectively. At low x , a Ti atom introduces two deep impurity bands near the CB edge of $c\text{-Si}_3\text{N}_4$ and the direct gap is reduced to 2.1 eV. Inspection of the wave functions reveals that the impurity bands consist of mainly the $\text{Ti-}3d(xy, yz, zx)$ orbitals with considerable mixing from the $\text{Si-}3s$ and $\text{Si-}3d$ orbitals. States with significant $\text{Ti-}3d(x^2-y^2, 3z^2-r^2)$ components are at a much higher energy of 5.7 eV (not shown in Fig. 5), and also mix with Si orbitals. As x increases, the ‘‘impurity bands’’

grow and merge with the CB with a concomitant reduction in E_g . This brings the exciting possibility of adjusting the direct E_g in this system by proper mixing. At $x=0.44$, the gap disappears and an insulator-to-metal transition is realized. Beyond $x=0.44$, the solid solution is a metal all the way up to $x=1.0$. The x dependence of E_g is shown in Fig. 7, which shows the relationship is not linear. Since the local density-functional theory generally underestimates the E_g of an insulator, and since the calculated result can also be affected by a variational and basis set effect as demonstrated recently by Bagayoko, Zhao, and Williams in several crystals,¹⁹ the precise value of x for metal-insulator transition in $\text{Si}[\text{Si}_{1-x}\text{Ti}_x]_2\text{N}_4$ may be somewhat uncertain.

IV. DISCUSSIONS

The theoretical prediction of the spinel phase of $c\text{-Ti}_3\text{N}_4$ and SiTi_2N_4 naturally leads to the question on how they might be prepared in laboratory. On the basis of past experience in the synthesis of related materials, it is our opinion that a high-temperature route is probably not feasible since direct nitridation of metallic Ti at high temperatures usually ends up with TiN in rocksalt structure. Even for the N_2 pressure above 100 MPa as in the case of self-propagating high-temperature synthesis, no higher nitrides of Ti, Zr, and Hf have been synthesized.²⁰ In the traditional ‘‘heat and beat’’ methods, it is difficult for the Ti ion to settle in a tet environment. Physical vapor deposition process as represented by reactive sputtering is not likely to succeed either because it will create too many defect structures and the materials more likely will end as $\text{Ti}_3\Box\text{N}_4$ rather than $c\text{-Ti}_3\text{N}_4$. Johansson *et al.* had tried to synthesize higher nitrides of Ti, Hf and Zr by dual beam deposition process.⁵ They obtained Hf_3N_4 and Zr_3N_4 in a defective rocksalt structure, but not Ti_3N_4 . Fix *et al.* have shown that Zr_3N_4 and Hf_3N_4 films can be prepared by chemical vapor deposition on various substrates.⁷ There were several other reports on the synthesis of TiN_x with $x>1$ by metallorganic or inorganic precursor decomposition, but no spinel Ti_3N_4 have thus far been reported. A trial to prepare Si-Ti nitrides from precursors was reported by Narula *et al.*²¹ They obtained a mixture of rocksalt TiN with $\alpha\text{-}$ and $\beta\text{-Si}_3\text{N}_4$, not the spinel phase. If these crystals can ever be synthesized, it probably has to be at low temperatures and with a very careful control of N_2 partial pressure using suitable precursor agents. The use of NH_3 and laser illumination or plasma treatment of N_2 may enhance the nitridation. Too high a pressure may result in the defective structure since the equilibrium volume of $\text{Ti}_3\Box\text{N}_4$ is smaller than that of $c\text{-Ti}_3\text{N}_4$. Lastly, we notice the predicted lattice constant of $c\text{-Ti}_3\text{N}_4$ is about twice that of TiN in rocksalt structure. TiN can therefore be a good substrate on which $c\text{-Ti}_3\text{N}_4$ can be grown epitaxially.

The calculated properties of $c\text{-Ti}_3\text{N}_4$, $c\text{-SiTi}_2\text{N}_4$ and its solid solutions suggest a number of interesting applications. Before these materials are actually synthesized and tested, the suggested applications are admittedly speculative and may even be premature. First, these are super hard materials and as such, can be used as cutting tools and protective coatings. They should be more oxidation resistant than TiN, similar to Si_3N_4 as a structural ceramic. Another important area is to use them as diffusion barrier and adhesion pro-

motor in semiconductor technology. c - SiTi_2N_4 , with its strong covalent bonding and no vacancy sites, can be highly resistant to the interdiffusion of impurity ions or self-diffusion. Its metallic properties can ensure a low electric resistivity and perhaps a higher thermal conductivity. The presence of Si should make it easier to integrate into the existing Si-based device materials similar to SiO_2 and Si_3N_4 . Solid solutions $\text{Si}[\text{Si}_{1-x}\text{Ti}_x]_2\text{N}_4$ exhibit insulator-to-metal transition and the direct band gap can be adjusted to the desired value by suitable mixing of Ti to Si. This special feature offers a tremendous opportunity for application in certain semiconductor technology where the size of the gap plays a crucial role. The materials are expected to have higher dielectric constants since it has a small band gap,¹² and may replace SiO_2 as the insulating layer in the MOSFET devices. The ever-shrinking submicron size of microelectronic devices will eventually reach the fundamental limit of SiO_2 as a gate oxide,²² and other viable alternative must be found. Lastly, the ideal lattice matching between TiN and c - Ti_3N_4 implies that many of the applications using TiN can be replaced with c - Ti_3N_4 which is an insulator rather than a metal.

V. CONCLUSIONS

We have used an *ab initio* method to predict the existence of the spinel phase of stoichiometric Ti_3N_4 . We have argued

that the existence of a stoichiometric spinel phase of Ti_3N_4 is a more likely model than the currently accepted defect model for Ti_3N_4 and TiN_x . Many previous diffraction analyses of TiN_x compounds failed to review the spinel structure because its lattice constant is almost twice of that of TiN in rocksalt structure. This situation may be the reason that they missed the model reported here. We also predict that spinel SiTi_2N_4 with Ti at the octahedral site and Si at the tetrahedral site should be stable. Electronic structure calculations show that c - Ti_3N_4 is a narrow gap semiconductor and c - SiTi_2N_4 to be a metal. Both crystals are super hard materials with strong covalent bonding. We further predict that by replacing Si by Ti at the tetrahedral sites of the spinel structure, the band gap of the solid solution can be adjusted and a metal-insulator transition should occur at the Ti to Si ratio of 0.44 for the octahedral sites. We further suggest possible routes of synthesis for these materials and also point out some potential applications of these predicted materials as structural ceramics as well as in semiconductor technology.

ACKNOWLEDGMENTS

Work at UMKC was supported by the U.S. Department of Energy under Grant No. DE-FG02-84DR45170. I. Tanaka was supported by the Grant-in-aid from Ministry of Education, Science, Sports and Culture of Japan.

*Author to whom correspondence should be addressed. Electronic address: chingw@umkc.edu

¹L. E. Toth, *Transition Metal Carbides and Nitride* (Academic, New York, 1971).

²J. L. Calais, *Adv. Phys.* **26**, 847 (1977).

³*Binary Alloy Phase Diagrams*, 2nd ed., edited by T. B. Massalski (ASM International, Materials Park, OH, 1990).

⁴H. A. Wriedt and J. L. Murray, *Bull. Alloy Phase Diagrams* **8**, 378 (1987).

⁵B. O. Johansson, H. T. G. Hentzell, J. M. E. Harper, and J. J. Cuomo, *J. Mater. Res.* **1**, 442 (1986).

⁶G. M. Brown and L. Maya, *J. Am. Ceram. Soc.* **71**, 78 (1988).

⁷R. Fix, R. G. Gordon, and D. M. Hoffman, *Chem. Mater.* **3**, 1138 (1991); **5**, 614 (1993).

⁸C. G. Faltermeier, C. Goldberg, M. Jones, A. Upham, A. Knorr, A. Ivanova, G. Peterson, A. E. Kaloyeros, and B. Arkles, *J. Electrochem. Soc.* **145**, 676 (1998).

⁹D. Seyferth and G. Mignani, *J. Mater. Sci. Lett.* **7**, 487 (1988).

¹⁰F. S. Glasco, *Structure and Properties of Inorganic Solids* (Pergamon, New York, 1970), p. 219.

¹¹A. Zerr, G. Miehe, G. Serghiou, M. Schwarz, E. Kroke, R. Riedel, H. Fueß, P. Kroll, and R. Boehler, *Nature (London)* **400**,

340 (1999).

¹²S.-D. Mo, L. Ouyang, W. Y. Ching, I. Tanaka, Y. Koyama, and R. Riedel, *Phys. Rev. Lett.* **83**, 504 (1999).

¹³W. Y. Ching, *J. Am. Ceram. Soc.* **73**, 3135 (1990).

¹⁴P. Hohenberg and W. Kohn, *Phys. Rev.* **136**, B864 (1964); W. Kohn and L. J. Sham, *Phys. Rev.* **140**, A1133 (1965).

¹⁵S.-D. Mo and W. Y. Ching, *Phys. Rev. B* **54**, 16 555 (1996).

¹⁶R. S. Mulliken, *J. Am. Chem. Soc.* **23**, 1833 (1955).

¹⁷R. Ahuja, O. Eriksson, J. M. Wills, and B. Johansson, *Phys. Rev. B* **53**, 3072 (1996).

¹⁸W. Wolf, P. Podloucky, T. Antretter, and E. D. Fisher, *Philos. Mag. B* **79**, 839 (1999).

¹⁹D. Bagayoko, G. L. Zhao, J. B. Fan, and J. T. Wong, *J. Phys.: Condens. Matter* **10**, 5645 (1999); G. L. Zhao, D. Bagayoko, and T. D. Williams, *Phys. Rev. B* **60**, 1563 (1999).

²⁰A. G. Merzhanov and S. Yu. Sharivker, *Materials Science of Carbides, Nitrides and Borides* (Kluwer Academic, Dordrecht, The Netherlands, 1999), p. 205.

²¹C. K. Narula, B. G. Demczyk, P. Czubarow, and D. Seyferth, *J. Am. Ceram. Soc.* **78**, 1247 (1995).

²²D. A. Muller, T. Sorsch, S. Moccio, F. H. Baumann, K. Evans-Lutterod, and G. Timp, *Nature (London)* **399**, 758 (1999).